Oxyhalogen−Sulfur Chemistry: Oxidation of *N*-Acetylcysteine by Chlorite and Acidic Bromate

James Darkwa*

Department of Chemistry, University of the Western Cape, Bellville 7535, South Africa

Rotimi Olojo, Olufunke Olagunju, Adenike Otoikhian, and Reuben Simoyi*,†

Department of Chemistry, Portland State University, P.O. Box 751, Portland, Oregon 97207-0751

Received: April 11, 2003; In Final Form: July 17, 2003

The kinetics and mechanism of the oxidation of an important organosulfur antioxidant, *N*-acetylcysteine, by chlorite and acidified bromate have been studied. In both cases, the final product is *N*-acetylcysteinesulfonic acid without cleavage of the C−S bond to form sulfate. There was also no evidence for the formation of *N*-chloramine nor *N*-bromamine as has been observed with other aminothiols such as taurine. *N*-Acetylcysteine was oxidized via a stepwise S-oxygenation process in which consecutively a sulfenic and a sulfinic acid were formed before formation of the cysteic acid product. The stoichiometry of the chlorite-*N*-acetylcysteine was experimentally deduced to be $3ClO_2^- + 2(CH_3CO)HNCH(CO_2H)CH_2SH \rightarrow 3Cl^- + 2(CH_3CO)HNCH(CO_2H)CH_2SO_3H$. The reaction is characterized by an immediate and rapid production of chlorine dioxide without a measurable induction period. This is because the oxidation of *N*-acetylcysteine by chlorine dioxide is slow enough to allow for the chlorine dioxide to instantly accumulate without the induction period that characterizes most chlorite oxidations of organosulfur compounds. The global reaction dynamics for this reaction can be described fully by a truncated mechanism that utilizes only 8 reactions. The stoichiometry of the bromate-*N*-acetylcysteine reaction at stoichiometric ratios was deduced to be $BrO_3^- + (CH_3CO)HNCH(CO_2H)CH_2SH \rightarrow Br^- + (CH_3CO)HNCH(CO_2H)CH_2SO_3H$, while in excess bromate it was deduced to be $6BrO_3^- + 5(CH_3CO)HNCH(CO_2H)CH_2SH + 6H^+ \rightarrow 3Br_2 + 5(CH_3CO)HNCH(CO_2H)CH_2SO_3H + 3H_2O$. This reaction proceeded with a prolonged induction period which gave way to a sudden formation of bromine. The rate of reaction between aqueous bromine and *N*-acetylcysteine is diffusion-limited which indicated that the end of the induction period coincided with a complete oxidation of *N*-acetylcysteine. The reaction was successfully modeled by the use of a reaction network made up of 12 elementary reactions. Despite their different physiological effects, both cysteine and *N*-acetylcysteine are oxidized by oxyhalogens via the same S-oxygenation pathway and gave the same oxidation metabolites and final product.

Introduction

Essential for growth and proliferation of all living organisms, sulfur forms an important and integral part of all living structures. The occurrence of sulfur mainly in the form of amino acids makes it the third most abundant macromineral on the basis of percentage of total body weight in human.[1] These sulfur-containing amino acids include cysteine, cystine, methionine, taurine, hypotaurine, and homocysteine. Deficiency or overproduction in these compounds can lead to several pathological diseases as observed with HIV patients who suffer an increased risk when deficient in sulfur-containing amino acids (SAAs).[2−4] Sulfur in most organic configurations is nucleophilic, and nucleophilic atoms are normally susceptible to metabolic activation via an oxidative pathway. The oxidative metabolism and transformations of sulfur compounds therefore become very vital to proper diagnosis and treatments of many diseases. There are many clinical trials involving sulfur compounds with promising therapeutic effects in the treatment of conditions such as chronic pancreatitis, cancer, diabetes, AIDS,[5,6] and arthritis. Responses to inflammatory stimuli are known to be influenced by dietary intake of many sulfur compounds such as glutathione and the metabolic precursor of cysteine: *N*-acetylcysteine, an established antioxidant.[5,7]

N-Acetylcysteine is a derivative amino acid of cysteine with an acetyl group attached to the nitrogen atom. It is a powerful antioxidant capable of acting as an antitoxin to compounds such as acrolein commonly found in cigarette smoke,[8,9] bromobenzene,[10] the toxic herbicide paraquat,[11,12] as well as the side effects of anti-cancer drugs cyclophosphamide and adrimycin. Its powerful antioxidant properties are based in its ability to effectively scavenge free radicals which are byproducts of normal metabolic activities.[13] Over production of free radicals often leads to DNA damage and cellular injuries which are now known to play a major role in the process of aging. The sulfur and sulfhydryl groups contained in *N*-acetylcysteine and its derivative, glutathione, are believed to be responsible for their ameliorating roles during inflammatory processes. Methionine and cysteine are known precursors of glutathione, which plays an important role in free radical defenses.[14] *N*-Acetyl-L-cysteine is considered a better precursor of glutathione than either cysteine or methionine because it retains about six times more of its sulfur group during the digestion process compared to cysteine.[15] Oral administration of *N*-acetylcysteine increases

* Authors to whom correspondence should be addressed.
† E-mail: rsimoyi@pdx.edu.

10.1021/jp0349841 CCC: $25.00
Published on Web 10/25/2003

intracellular cysteine and glutathione levels in addition to its metabolic transformation into cystine and methionine,[16] while dietary supplement of *N*-acetylcysteine is a better source of glutathione than orally ingesting glutathione. This greater efficiency is important since cellular glutathione levels tend to drop significantly with age. It has been strongly argued that supplemental *N*-acetylcysteine may have an anti-aging effect by increasing glutathione levels in the liver, lungs, kidneys, and bone marrow. Studies have suggested that HIV-positive patients could lose as much as 10 g of cysteine per day, resulting in heavy depletion of sulfur and a large drain of the glutathione pool.[17,18]

Our research interest has largely focused on the kinetics and mechanistic details of the oxidation of small organic sulfur compounds by oxyhalogens. Some of our recent work was on the oxidation kinetics of cysteine with chlorite ions. The sulfur centers of these organosulfur compounds are highly susceptible to oxidation by various biological oxidants such as $O_2^{\bullet-}$, HOCl, and H_2O_2. HOCl, for example, is a bactericidal compound formed by activated neutrophils during inflammation.[19] Excessive production of HOCl causes damage to tissues at the site of neutrophil accumulation. The antioxidant properties of many thioethers and thiols such as *N*-acetylcysteine, cysteine, and glutathione are known to be very effective against the deleterious effects of excessive HOCl formation. Favorable reactions from thiols with the accumulating HOCl can avert alterations in regulatory and signaling pathways in cells that are exposed to neutrophils oxidants.[20]

Despite the importance of S-oxygenation for the study of sulfur metabolism, very few studies have been performed on the oxidation mechanisms of the important biological thiols, thioamides, and dithiocarbamates. The chemical and biological properties of these sulfur compounds depend on the nature of the substituents on the organic backbone of the molecule. Subtle differences in substitution can impart vastly different degrees of physiological activity. For example, while α-naphthylthiourea produces pulmonary edema in rats, diphenylthiourea is quite innocuous. Despite their similarities, cysteine and *N*-acetylcysteine exert very different physiological effects. The S-oxygenation mechanism for cysteine has been studied by us in our laboratories,[21] but there are no corresponding studies for *N*-acetylcysteine, which is the more important and widely used aminothiol. In this manuscript, we intend to report on the oxidation of *N*-acetylcysteine by some selected oxyhalogens. The knowledge of the selectivity of these oxidants toward *N*-acetylcysteine will help in the understanding of some of its relevant physiological properties as well as explain the differences when compared with its analogue, cysteine. The relative rates and the ease of oxidation of the sulfur centers to possible sulfur oxo-acids should establish correlation with their antioxidant properties in physiological environments.

Experimental Section

Materials. The following analytical grade chemicals were purchased from Fisher Scientific and used without further purification: sodium chlorate, sodium bromate, sodium perchlorate, bromine, oxalic acid, sodium carbonate, perchloric acid (70%), potassium iodide, hydrochloric acid, sodium thiosulfate, starch, and sulfuric acid. *N*-Acetylcysteine (Sigma-Aldrich) was used without further recrystallization. Sodium chlorite (Aldrich) was recrystallized from its ca. 80% technical grade purity to ∼99% assay. This was carried out from a water−ethanol−acetone mixture, and crystals formed were dried over a period of one week in a desiccator. The recrystallized chlorite was standardized iodometrically by adding acidified potassium iodide. The liberated iodine was then titrated against sodium thiosulfate using freshly prepared starch as indicator and employing the following stoichiometries:[22]

$$ClO_2^- + 4I^- + 4H^+ \rightarrow 2I_2 + Cl^- + 2H_2O$$

$$I_2 + 2S_2O_3^{-2} \rightarrow 2I^- + S_4O_6^{2-}$$

Standardization of aqueous bromine solution was equally carried out using the method described above with the following stoichiometric reaction:

$$Br_2 + 2I^- \rightarrow I_2 + 2Br^-$$

The concentration of bromine was also determined by measuring the absorbance at 390 nm where the extinction coefficient of bromine had been deduced as 142 M^{-1} cm^{-1}.[23] Bromine solutions, being volatile, were kept capped and were standardized before each set of experimental runs. Chlorine dioxide was prepared by the standard method of oxidizing sodium chlorate in a sulfuric acid/oxalic acid mixture. The stream of chlorine dioxide produced was passed through sodium carbonate solution before being collected in ice-cold water at 4 °C at a pH of ∼3.5.

Standardization of ClO_2 was also accomplished by iodometric techniques using the following stoichiometries:

$$2ClO_2 + 10I^- + 8H^+ \rightarrow 5I_2 + 2Cl^- + 4H_2O$$

$$I_2 + 2S_2O_3^{-2} \rightarrow 2I^- + S_4O_6^{2-}$$

The results obtained were confirmed spectrophotometrically by using an absorptivity coefficient of ClO_2 of 1265 M^{-1} cm^{-1} at 360 nm.[24]

Methods. Stoichiometric determinations were carried out by mixing various oxidant/reductant ratios in stoppered volumetric flasks and scanning them spectrophotometrically for ClO_2 activity over a period of 24 h. Products formed from *N*-acetylcysteine oxidation by chlorite were characterized by ^1H NMR measurements using D_2O as solvent and internal standard (4.67 ppm). Reaction kinetics were followed on a Hi-Tech DX2 double mixing stopped-flow spectrophotometer for the oxidation of substrate by chlorite, chlorine dioxide, and bromine. Absorbance traces were obtained by following either the appearance or consumption of ClO_2 at 360 nm and the consumption of bromine at 390 nm. The slower oxidation by acidic bromate was monitored on a conventional Perkin-Elmer Lambda 2S UV−Vis spectrophotometer. All measurements were carried out at 25.0 ± 0.5 °C with ionic strength maintained at 1.0 M using $NaClO_4$. Qualitative tests for the presence of sulfate were performed using $BaSO_4$ precipitation as indicator. The stoichiometries of reactions involving chlorine dioxide and bromine were determined by pure titration of the oxidant into excess substrate with starch as indicator. Starch prepared with mercuric iodide as a preservative gave a deep blue-black color with excess chlorine dioxide and bromine as oxidants.[22]

Results

Stoichiometry of Chlorite Oxidation. The stoichiometry of the reaction between *N*-acetylcysteine and chlorite in slightly acidic media was experimentally deduced to be

$$3ClO_2^- + 2(CH_3CO)HNCH(CO_2H)CH_2SH \rightarrow 3Cl^- + 2(CH_3CO)HNCH(CO_2H)CH_2SO_3H \quad (R1)$$

Stoichiometry of R1 was deduced by finding the highest chlorite/*N*-acetylcysteine ratio that could be used without the production of chlorine dioxide after an incubation period of more than 24 h. This ratio corresponds to the point where any further addition of chlorite will lead to generation of ClO_2. Chlorine dioxide is generated from the disproportionation of excess chlorite after all the reducing substrate has been consumed.[25] Confirmation of the results obtained was carried out by titrimetric analysis using excess chlorite as oxidant and back-titrating the oxidizing power of the unreacted oxidant. A linear plot could then be generated of titer versus amount of oxidant and extrapolated to find amount of oxidant for zero titer.

Tests with $BaCl_2$ revealed no evidence for the formation of sulfate under any oxidizing conditions, indicating that the terminal carbon−sulfur bond is not cleaved during oxidation at the sulfur center. The final oxidation product was 2-acetylamino-3-sulfo-propionic acid (*N*-acetylcysteine sulfonic acid) at all oxidizing conditions. To fully characterize the *N*-acetylcysteine oxidation by chlorite, comparative oxidation by chlorine dioxide was studied. The reaction also gave *N*-acetylcysteine sulfonic acid as its major product with no formation of sulfate according to the following stoichiometry:

$$6ClO_2 + 5(CH_3CO)HNCH(CO_2H)CH_2SH + 3H_2O \rightarrow 6Cl^- + 5(CH_3CO)HNCH(CO_2H)CH_2SO_3H + 6H^+ \quad (R2)$$

The stoichiometric ratio was confirmed by UV−Vis spectrophotometry as the ratio just before the appearance of excess ClO_2 at its λ_{max} of 360 nm.

Stoichiometry of Bromate Oxidation. The reaction between *N*-acetylcysteine and acidic bromate gave a stoichiometry of 1:1 with the same organic product as in chlorite oxidation. The stoichiometry was derived as

$$BrO_3^- + (CH_3CO)HNCH(CO_2H)CH_2SH \rightarrow Br^- + (CH_3CO)HNCH(CO_2H)CH_2SO_3H \quad (R3)$$

Excess bromate, after complete oxidation of *N*-acetylcysteine according to stoichiometry R3 will react with the bromide product to produce bromine:[26]

$$BrO_3^- + 5Br^- + 6H^+ \rightarrow 3Br_2 + 3H_2O \quad (R4)$$

In any situation with excess bromate, yellow aqueous bromine is obtained after an induction period due to the extraneous reaction of R4. A titrimetric analysis was carried out to determine excess bromate in varying substrate/oxidant ratio via conversion of bromine generated to iodine and back-titrating I_2 against standard sodium thiosulfate using starch as indicator. A linear combination of reactions R3 and R4 (5R3 + R4) gave the stoichiometry of reaction in excess oxidant:

$$6BrO_3^- + 5(CH_3CO)HNCH(CO_2H)CH_2SH + 6H^+ \rightarrow 3Br_2 + 5(CH_3CO)HNCH(CO_2H)CH_2SO_3H + 3H_2O \quad (R5)$$

The amount of bromine formed was directly proportional to the initial reductant concentration. This is evident from data obtained with varying *N*-acetylcysteine concentrations where the amount of bromine formed was exactly 60% of the initial concentration of reductant (measured spectrophotometrically).

The direct reaction between aqueous bromine and *N*-acetylcysteine gave the following stoichiometry:

$$3Br_2 + (CH_3CO)HNCH(CO_2H)CH_2SH + 3H_2O \rightarrow 6Br^- + (CH_3CO)HNCH(CO_2H)CH_2SO_3H + 6H^+ \quad (R6)$$

Sulfate was not detected either in stoichiometry R6. This evidence suggests that the primary oxidation products from *N*-acetylcysteine with all the oxidants used in this work are formed via stepwise addition of oxygen to the sulfur center without any C−S bond cleavage. The formation of *N*-acetylcysteine sulfonic acid from chlorite oxidation of *N*-acetylcysteine was re-confirmed by ^1H NMR spectroscopy. Figure 1 shows spectrum A for pure *N*-acetylcysteine while spectrum B was taken after addition of chlorite as oxidant. Both spectra show the region 2.80−4.60 ppm taken at nearly neutral pH conditions using D_2O as solvent. The methyl protons on the acetyl group resonate around 2.0 ppm before and after oxidation by chlorite, suggesting that the reactions occurring are remotely across the acetyl group on the sulfur atom and no methyl protons coupling are present. Spectrum A shows a triplet around 4.62 ppm from the asymmetric proton H_a, a splitting arising from coupling of H_a with adjacent methylene protons H_b and H_c. The two methylene protons gave a complex doublet of a doublet split at about 3.00 ppm arising from unequal coupling between protons H_b and H_c with H_a. Dissimilar environment exists around proton H_a created by the adjacent asymmetric carbon. Upon addition

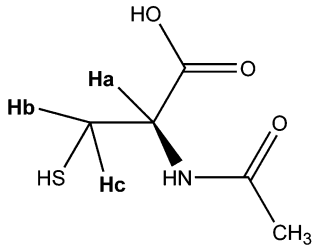

N-Acetylcysteine

of chlorite, there was a significant shift in the methylene proton resonance from ∼3.00 ppm to a new peak centered on ∼3.48 ppm, as shown in spectrum B. The downfield shift can be ascribed to the formation of the more electron-withdrawing sulfonic group upon oxidation of the sulfur center to a +4 oxidation state. The coupling constant of protons H_b and H_c in spectrum A is increased going to spectrum B due to increased dissimilarities between the two protons as a result of different electronic environments created by the bulkier sulfonic acid group. The NMR data obtained show a trend similar to that obtained from cysteine oxidation from an earlier study,[21] lending further support to the transformation of the thiol group to a stable sulfonic acid. The methyl carbonyl group attached to nitrogen is retained in the final product, as evidenced by the peak at 2.0 ppm in spectrum B.

Reaction Dynamics. *Chlorite Oxidation of N-Acetylcysteine.* The reaction of *N*-acetylcysteine with chlorite showed a rapid formation of chlorine dioxide at conditions of stoichiometric excess of the oxidant, chlorite. Figure 2 shows both immediate and monotonic formation of ClO_2, leading to its accumulation within 40 s for unbuffered reaction solutions. The pH of the reaction solution plunges from approximately 7.0 to 2.0 during this 40 s period. As the starting concentration of chlorite increases, the final concentration of ClO_2 increases as seen in traces a−f in Figure 2. Chlorite concentrations close to the stoichiometric ratios (3:2) showed two stages of ClO_2 formation

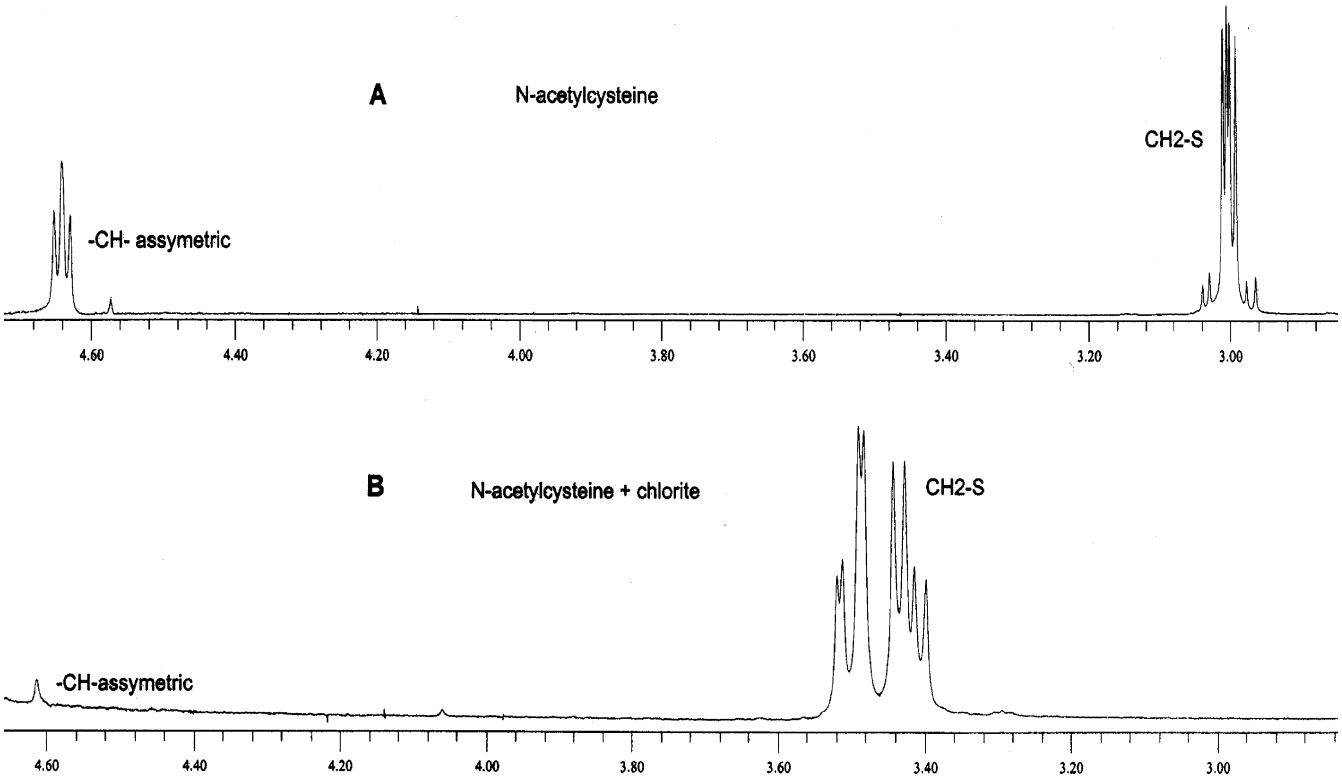

Figure 1. ^{1}H NMR spectrum of pure *N*-acetylcysteine (A) and that of the product of the reaction between *N*-acetylcysteine and chlorite (B). The downfield shift is expected due to the formation of the electron-withdrawing sulfonic acid group in *N*-acetylcysteinesulfonic acid. The bulkier sulfonic acid group also increases the coupling constants of the different interacting protons.

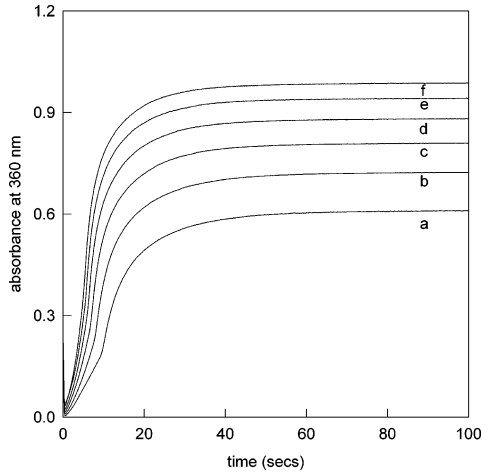

Figure 2. Absorbance traces at 360 nm for the oxidation of *N*-acetylcysteine by chlorite at varying oxidant concentrations in slightly acidic conditions. No attempt was made to control the pH in this series of experiments, and a rapid decrease in pH is observed at the beginning of the reaction. Formation of chlorine dioxide is almost instantaneous with its rate being proportional to the initial concentration of chlorite. $[NAC-CH_2SH]_0 = 0.001$ M. $[ClO_2^-]_0 =$ (a) 0.005 M; (b) 0.006 M; (c) 0.007 M; (d) 0.008 M; (e) 0.009 M; (f) 0.01 M.

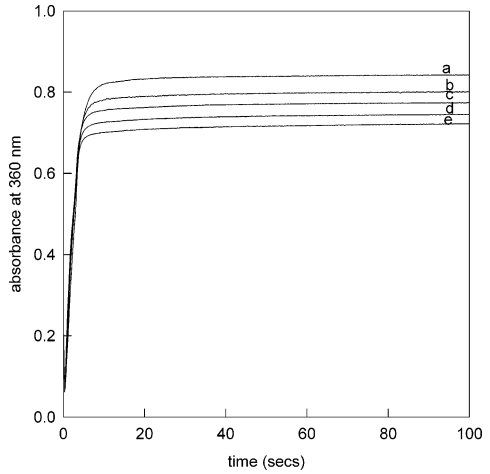

Figure 3. Effect of variation of acid on the rate of formation of chlorine dioxide. Surprisingly, higher acid concentrations produce lower chlorine dioxide concentrations. All experiments shown were performed $R = 10$. $[ClO_2^-]_0 =$ (a) 0.01 M. $[NAC-CH_2SH]_0 = 0.001$ M. $[H^+]_0 =$ (a) 0.003 M; (b) 0.0045 M; (c) 0.006 M; (d) 0.0075 M; (e) 0.009 M.

with a faster second step (see traces a, b, and c in Figure 2). In the presence of acid, there is a net decrease in the final concentration of ClO_2 generated as H^+ concentration increases, although the initial rates of all the reactions appear to be unaffected by changing acid concentrations as displayed in Figure 3. This inhibitory effect of acid on the final concentration of ClO_2 is inconsistent with acid effects on typical oxyhalogen reactions. Nearly all oxyhalogen reactions are catalyzed by acid,[27] suggesting that the observed inhibition in chlorine dioxide formation might be emanating from the chemistry of the substrate. However, changes in concentrations of the substrate produce greater effects on the dynamics of the reactions. Figure 4 shows a rapidly increasing initial rate of production of ClO_2 as the initial concentrations of *N*-acetylcysteine are increased. Upon further observation of the reactions shown in Figure 4, chlorine dioxide concentrations continued to increase, even after 24 h such that solution a, with the lowest amount of substrate, gave the highest chlorine dioxide concentrations and trace e, with the highest substrate concentrations, gave the lowest. Despite this, the total oxidizing power did not change, and one still obtained stoichiometry R1 from titrimetric techniques. This further chlorine dioxide formation is merely a thermodynamically favorable transformation of the oxychlorine species.[28] Total

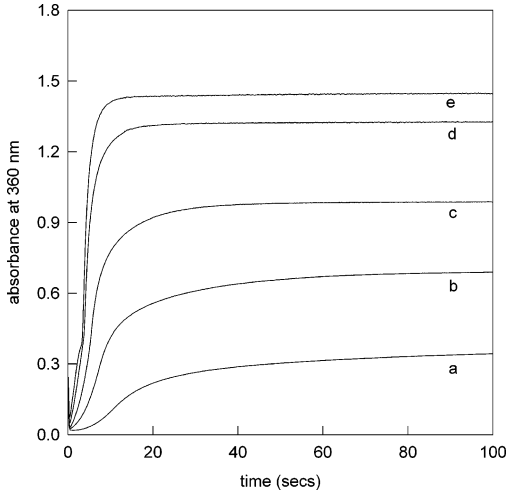

Figure 4. Effect of substrate variation. Higher substrate concentrations delivered higher chlorine dioxide concentrations. A much slower increase in chlorine dioxide concentrations was observed after the plateau shown, and this could be attributed to normal disproportionation of acidic chlorite solutions. The acid is a product of the reaction. $[ClO_2^-]_0 = 0.01$ M. $[NAC-CH_2SH]_0 =$ (a) 0.00025 M; (b) 0.0005 M; (c) 0.001 M; (d) 0.002 M; (e) 0.003 M.

consumption of the substrate will have occurred in the first 40 s of the reaction.

Chlorine Dioxide Oxidation of N-Acetylcysteine. The consumption of chlorine dioxide by *N*-acetylcysteine displayed a typical first-order dependence profile in excess reductant with slight increases in the initial rate of oxidant depletion as the concentration of ClO_2 increases. Figure 5a shows a series of reactions at stoichiometric excess of chlorine dioxide. These kinetics traces show a simple first-order dependence of oxidant concentrations. Since the reaction solutions were not buffered, the final pH was much lower due to the production of acid according to stoichiometry R2. The reaction was fast and essentially over within 10 s. The final residual amount of ClO_2 at the end of reaction corresponds to the difference between the starting concentration of ClO_2 and the amount of oxidant consumed by the substrate based on stoichiometry R2. Kinetics data taken while varying the substrate concentration (Figure 5b) also give first-order dependence on the concentration of substrate. A close examination of traces such as e in Figure 5b show what appears to be autoinhibition as the reaction proceeds. Acid, however, has a significant retardation effect on the oxidation of *N*-acetylcysteine by chlorine dioxide, as seen in Figure 5c. There is an inverse dependence of initial rate on acid at low concentrations of acid (see Figure 5c insert). This inverse acid dependence, however, prevails only at high acid concentrations, $[H^+]_0 > 0.01$ M. pH conditions below 2.0 support only protonated $HClO_2$ molecules with negligible amounts of dissociated chlorite anions.

Bromate Oxidation of N-Acetylcysteine. High acidic environments were employed for the bromate oxidation of *N*-acetylcysteine (pH < 2) which suggests both the amino and the thiol centers will be highly protonated:

$$(CH_3CO)H_2N^+CH(CO_2^-)CH_2SH + H^+ \rightleftharpoons (CH_3CO)H_2N^+CH(CO_2^-)CH_2S^+H_2 \quad (R7)$$

Bromate oxidations are very slow to negligible in pH conditions above 3.0. Contrary to the reaction dynamics displayed by the chlorite−*N*-acetylcysteine reaction, the corresponding oxidation by bromate gives a long quiescent induction period with no

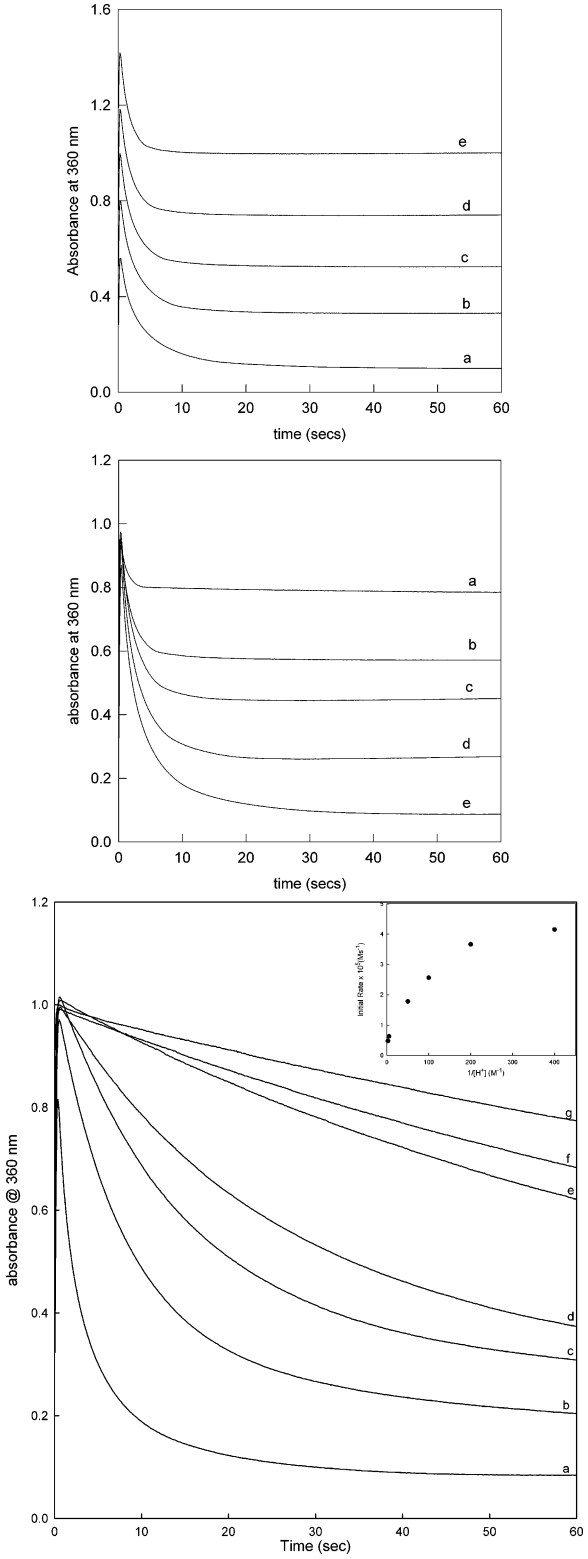

Figure 5. (a) Consumption of chlorine dioxide by *N*-acetylcysteine in unbuffered solutions. The stoichiometric equivalent of chlorine dioxide was achieved within 30 s. $[NAC-CH_2SH]_0 = 0.00025$ M. $[ClO_2]_0 =$ (a) 0.00069 M; (b) 0.00092 M; (c) 0.00115 M; (d) 0.00138 M; (e) 0.00161 M. (b) Variation of *N*-acetylcysteine in its oxidation by chlorine dioxide in unbuffered solutions. Higher *N*-acetylcysteine concentrations show what appears to be slight autoinhibition. The pH of the solution decreases as the reaction proceeds (see stoichiometry R2). $[ClO_2]_0 =$ (a) 0.00115 M. $[NAC-CH_2SH]_0 =$ (a) 0.0001 M; (b) 0.0002 M; (c) 0.0003 M; (d) 0.0004 M; (e) 0.0005 M. (c) Effect of acid on the *N*-acetylcysteine−chlorine dioxide reaction. Acid is strongly inhibitory. $[ClO_2]_0 = 0.00095$ M. $[NAC-CH_2SH]_0 = 0.0025$ M $[H^+]_0 =$ (a) 0.0 M; (b) 0.0025 M; (c) 0.01 M; (d) 0.02 M; (e) 0.1 M; (f) 0.4 M.

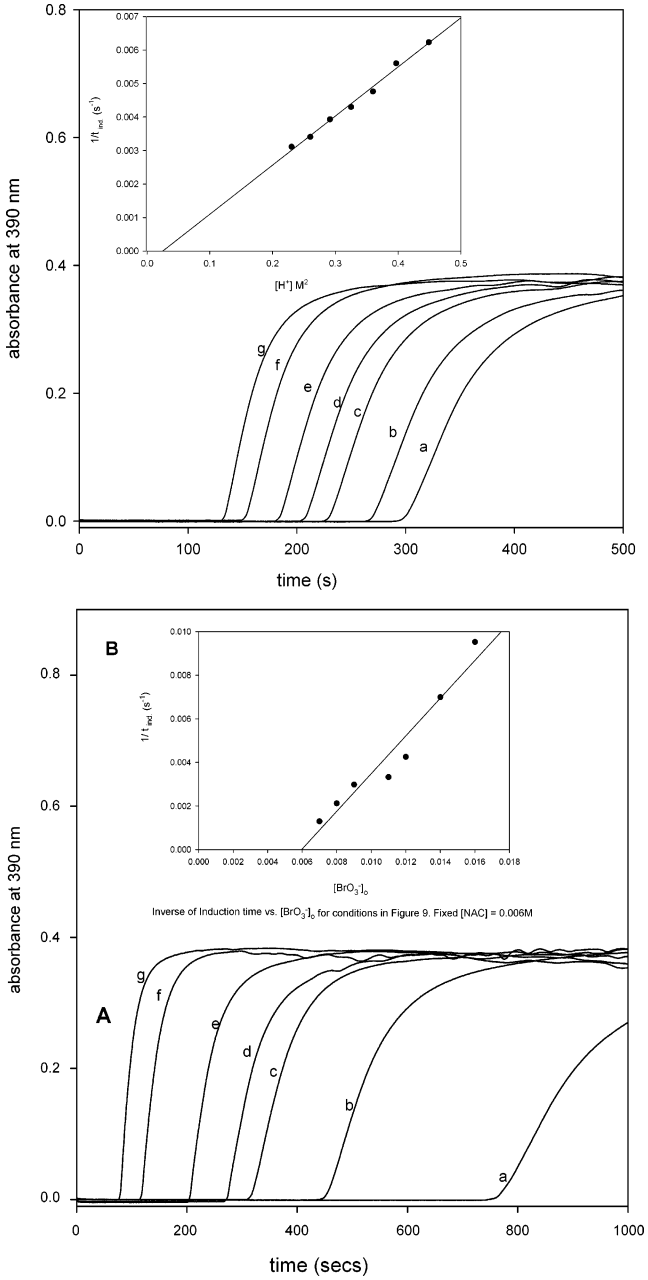

Figure 6. (a) Absorbance traces at 390 nm showing the effect of acid on the *N*-acetylcysteine−bromate reaction. There is an inverse square acid dependence on the induction period (see insert). $[NAC-CH_2SH]_0 = 0.004$ M. $[BrO_3^-]_0 = 0.01$ M. $[H^+]_0 =$ (a) 0.48 M; (b) 0.51 M; (c) 0.54 M; (d) 0.57 M; (e) 0.60 M; (f) 0.63 M; (g) 0.67 M. (b) Same experiments as in Figure 6a with bromate variations. There is a simple inverse relationship between the initial bromate concentrations and the induction period (see insert). At constant substrate concentrations, final amount of bromine formed is invariant (see stoichiometry R5). $[NAC-CH_2SH]_0 = 0.006$ M. $[H^+]_0 = 0.01$ M. $[BrO_3^-]_0 =$ (a) 0.007 M; (b) 0.008 M; (c) 0.009 M; (d) 0.011 M; (e) 0.012 M; (f) 0.014 M; (g) 0.016 M.

change in the reaction indicators: redox potential, pH, conductivity, or visible color change. This quiescent induction period gives way to a sudden and very rapid production of bromine coupled to an increase in redox potential from 600 mV to approximately 900 mV with a calomel reference (offset 201 mV). The induction period is heavily dependent on the initial reagent concentrations as well as the ratio *R* of oxidant to reductant: $[BrO_3^-]_0/[N\text{-acetylcysteine}]_0$. As expected for any oxyhalogen-driven oxidation, acid exerts a most powerful effect on both the induction period and the rate of formation of

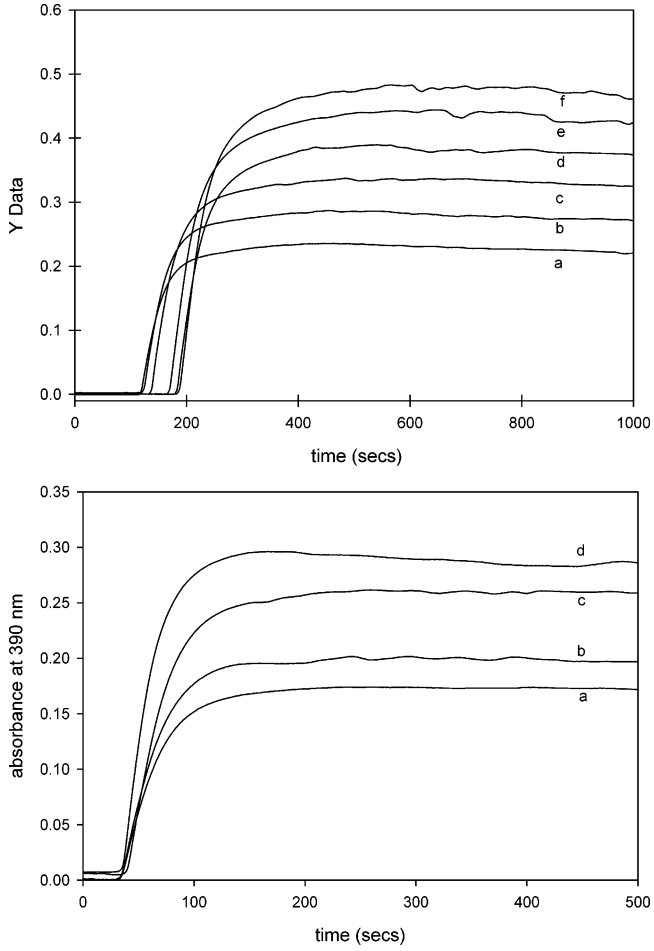

Figure 7. (a) Higher *N*-acetylcysteine concentrations at fixed bromate concentrations gave longer induction periods which suggests that the complete oxidation of the substrate is a prerequisite for the formation of aqueous bromine. $[H^+]_0 = 0.60$ M. $[BrO_3^-]_0 = 0.01$ M $[NAC-CH_2SH]_0 =$ (a) 0.0025 M; (b) 0.003 M; (c) 0.0035 M; (d) 0.004 M; (e) 0.0045 M; (f) 0.005 M. (b) At excess oxidant concentrations, *R* 0.20; there is no change in induction period. Higher *N*-acetylcysteine concentrations gave higher bromine production rates as well as higher bromine concentrations at the end of the reaction. $[H^+]_0 = 0.24$ M. $[BrO_3^-]_0 = 0.05$ M $[NAC-CH_2SH]_0 =$ (a) 0.0017 M; (b) 0.0021 M; (c) 0.0025 M; (d) 0.0029 M.

bromine at the end of the induction period (see Figure 6a). The end of the induction period is very sharp and precise, and the length of the quiescent period can be correlated with initial reagent concentrations. The insert in Figure 6a shows that there is an inverse square acid dependence on the length of the induction period. All reaction runs observed in Figure 6a were at $R = 2.5$, which represents stoichiometric excess of oxidant leading to stoichiometry R5. Thus final bromine concentration for all seven experimental runs were the same. When $R < 1$, no bromine formation is observed and induction period goes to infinity. This is only possible if the reaction of bromine with *N*-acetylcysteine is so rapid that formation of bromine would denote complete consumption of *N*-acetylcysteine. This behavior can be utilized and tested as a complementary test for stoichiometry R3 from the data in Figure 6b. Similar effect was observed with variations in bromate concentration (see Figure 6b), as increasing $[BrO_3^-]_0$ shortens the induction period without a change in the final bromine concentration. A plot of $1/t_{ind}$ vs $[BrO_3^-]_0$ (Figure 7b insert) gave a linear dependence. The intercept on the $[BrO_3^-]_0$ axis is the limiting concentration where the corresponding induction time just becomes finite (or just goes to infinity). Formation of Br_2 occurs only at concentrations

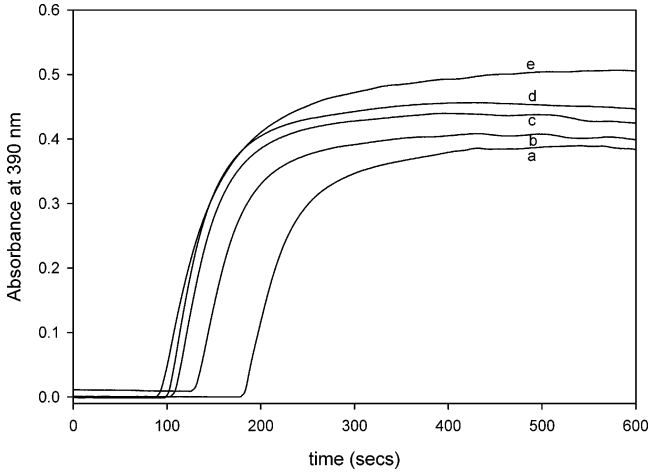

Figure 8. Effect of bromide on the oxidation of *N*-acetylcysteine by bromate. Low and trace amounts of bromate noticeably catalyzed the reaction while further increases in bromide concentrations did not deliver as visible an effect. $[H^+]_0 = 0.24$ M. $[BrO_3^-]_0 = 0.01$ M. $[NAC-CH_2SH]_0 = 0.004$ M. $[Br^-]_0 =$ (a) 0.0 M; (b) 0.0002 M; (c) 0.0006 M; (d) 0.0008 M; (e) 0.0012 M.

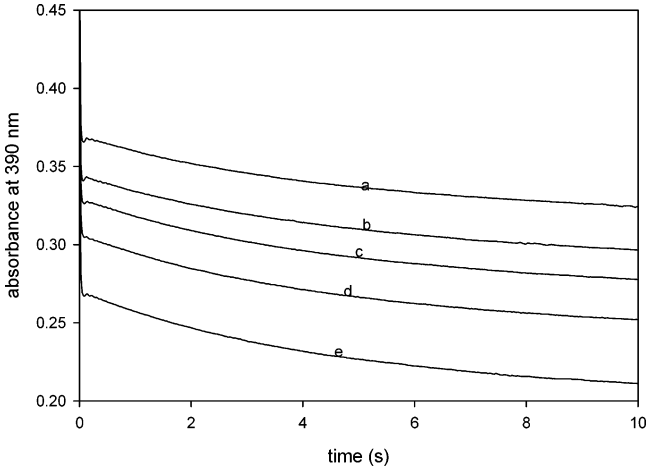

Figure 9. Absorbance traces at 390 nm showing the rapid bromine−*N*-acetlycysteine reaction. The reaction is so fast that our stopped-flow ensemble can only catch the last 20% of the reaction. $[Br_2]_0 = 0.005$ M. $[NAC-CH_2SH]_0 =$ (a) 0.005 M; (b) 0.00563 M; (c) 0.000625 M; (d) 0.000688 M; (e) 0.0075 M.

greater than the limiting $[BrO_3^-]_0$ value after stoichiometry R3 has been satisfied. The initial concentration of *N*-acetylcysteine used for all the experiments in that set was 0.006 M. The intercept of 0.006 M bromate as the imiting concentration confirms a 1:1 stoichiometry as described in reaction R3. The effect of *N*-acetylcysteine on the induction period is more complex than for bromate and acid (Figures 7a and 7b). In Figure 7a, *R* is varied from 2 to 4; within this range the induction period decreases, but not in any simple functional form. The effect of the substrate concentrations on the induction period wanes as the value of *R* increases. By running a series of reactions at high ratios, $30 > R > 17$, one notices in Figure 7b that the induction period becomes invariant. However, in both cases, Figures 7a and 7b, the rate of formation and amount of bromine formed is directly proportional to the initial concentration of substrate, as predicted by stoichiometry R5. The effect of bromide ion can be evaluated at two separate conditions: low bromide (1−100 μM) and high bromide (>200 μM). At low bromide concentrations, bromide ions exert a powerful catalytic effect on the rate of the reaction by dramatically shortening the induction period (see Figure 8); but as bromide is further increased, this catalytic effect is decreased and instead an increase in the final bromide concentration due to the effects of reaction R4 is observed. However, at no time is the effect of bromide ever inhibitory.

N-Acetylcysteine Oxidation by Aqueous Bromine. Oxidation of *N*-acetylcysteine by bromine was extremely fast ,and the first step of the two-staged reaction was essentially complete within one-hundredth of a second (see Figure 9). An estimated lower-limit diffusion-controlled second-order rate constant for the first step is $(5.0 \pm 1.5) \times 10^7$ M^{-1} s^{-1}. The second step is less rapid, and it involves the conversion of the intermediate formed to the final oxidation product—*N*-acetylcysteine sulfonic acid. An examination of the data in Figure 9 shows that there is an initial diffusion-controlled first step in which 2 moles of bromine are consumed for each mole of *N*-acetylcysteine. This suggests that the oxidation to the sulfinic acid stage is very facile:

$$2Br_2 + (CH_3CO)HNCH(CO_2H)CH_2SH + 2H_2O \rightarrow 4Br^- + (CH_3CO)HNCH(CO_2H)CH_2SO_2H + 4H^+ \quad (R8)$$

Such rapid kinetics have been observed previously on reactions involving an electrophilic attack by bromine on a sulfur center.[23]

Global Reaction Dynamics. *Chlorite−N-Acetylcysteine Reaction.* The formation of HOCl from *N*-acetylcysteine is the first step in the series of reactions involved in *N*-acetylcysteine oxidation to form *N*-acetylcysteine sulfonic acid. Important intermediates that are formed include the sulfenic and sulfinic acids.

$$ClO_2^- + \text{Red} \rightarrow HOCl + \text{Ox} \quad (R9)$$

HOCl is a reactive species whose rapid reaction with excess chlorite produces chlorine dioxide:[29]

$$2ClO_2^- + HOCl + H^+ \rightarrow 2ClO_2 + Cl^- + H_2O \quad (R10)$$

The ClO_2 generated in the reaction R10 can oxidize any available reducing species that is available in solution:

$$2ClO_2 + \text{Red} \rightarrow 2ClO_2^- + \text{Red}^{2+} \quad (R11)$$

The effective coupling of reactions R9, R10, and R11 by virtue of their comparable magnitudes in rate is responsible for the exotic dynamics observed in these reaction systems. The small organic backbone of *N*-acetylcysteine limits the number of possible intermediates that can be generated in the reaction mixtures leading to a much simpler mechanism when compared to the common exotic behavior that often characterizes many sulfur-based oxidations. Transient intermediates expected during the course of oxidation of *N*-acetylcysteine include dimers of the form RS−SR, sulfenic acids, RSOH, and sulfinic acids, RSO_2H,[30] prior to the formation of the stable sulfonic acid, RSO_3H; where R is the *N*-acetylcysteine carbon backbone. On the other hand, important oxyhalogen reactions may produce HOCl, Cl^-, and ClO_2 and other less significant oxyhalogen species.[29] The major oxidizing species involved in all the reactions are HOCl, ClO_2^-, and ClO_2(aq). A two-electron reduction of ClO_2^- is expected to produce HOCl as the reactive species which is used for further oxidations of the substrates.

Mechanism. Acidified chlorite solutions produce chlorine dioxide upon prolonged standing. The kinetics of this transformation, are, however, very slow. Our reaction shows an almost instantaneous formation of chlorine dioxide upon mixing *N*-acetylcysteine with chlorite. The formation of chlorine dioxide from acidified chlorite, in this reaction system, must be catalyzed by the oxidation of *N*-acetylcysteine through the formation of

the necessary reactive intermediate (HOCl) which is needed for the oxidation of chlorite. The rapid formation of chlorine dioxide, combined with the absence of a discernible induction period before its formation implies that the reactions that might consume chlorine dioxide are much slower than those that produce it. The initial step in any nonradical oxidation by chlorite involves a 2-electron addition on the chlorine center to form hypochlorous acid:[24]

$$ClO_2^- + 3H^+ + 2e^- \rightarrow HOCl + H_2O \qquad (R12)$$

Hypochlorous acid, formed in reaction R12 can further oxidize the organic substrates or oxidize chlorite to form chlorine dioxide. The relative rates of these two processes will determine whether there will be instant chlorine dioxide formation, delayed formation, or no formation at all. In excess reductant, in which we expect all the oxychlorine species to be reduced to chloride, formation of chlorine dioxide will not be expected unless the rate of reduction of the chlorine dioxide formed is exceedingly slower than the reactions that form chlorine dioxide.[31] Although we expect intermediate sulfur species to assert themselves along the oxidation pathway, at the beginning of the reaction, however, only *N*-acetylcysteine is present and will be the dominant reducing species that initiates reaction R12. A two-electron oxidation of *N*-acetylcysteine should produce the unstable sulfenic acid:

$$NAC{-}CH_2SH + ClO_2^- \rightarrow NAC{-}CH_2SOH + OCl^- \qquad (R13)$$

followed by the diffusion-limited protonation reaction:

$$OCl^- + H^+ \rightarrow HOCl \qquad (R14)$$

In the presence of further oxidant, the sulfenic acid should be easily oxidized to the more stable sulfinic acid:

$$NAC{-}CH_2SOH + H_2O \rightarrow NAC{-}CH_2SO_2H + 2H^+ + 2e^- \qquad (R15)$$

The oxidant could either be chlorite, hypochlorous acid, aqueous chlorine, or chlorine dioxide. Since any further two-electron reduction of hypochlorous acid produces chloride, the standard chlorine hydrolysis reaction should become viable and produce aqueous chlorine:[32]

$$HOCl + H^+ + Cl^- \rightleftharpoons Cl_2(aq) + H_2O \qquad (R16)$$

The oxidizing power of the oxychlorine species does not change due to equilibrium R16. While aqueous chlorine oxidizes mainly through electron transfer followed by hydrolysis, hypochlorous acid oxidizes by oxygen atom transfer. If the rates of these two processes are vastly different, then one will expect a rapid change in reaction rate with pH. If the reaction with aqueous chlorine is much faster than that with hypochlorous acid, then both oxidations will be kinetically indistinguishable since reactions of type R13 + R14 will still be rate-determining.

Peintler et al have studied the reaction between chlorite and hypochlorous acid and found it to deliver rate laws and products that depend on pH and the relative ratios of chlorite to hypochlorous acid.[29] The predominant product in the pH range we studied appears to be chlorine dioxide:

$$HOCl + 2ClO_2^- + H^+ \rightleftharpoons 2ClO_2(aq) + Cl^- + H_2O \qquad (R10)$$

with negligible formation of chlorate (which is oxidatively inert). The exact mechanism of this composite reaction is still speculative, but it is now assumed to proceed through two steps:[33]

$$HOCl + ClO_2^- + H^+ \rightleftharpoons Cl_2O_2 + H_2O \qquad (R17)$$

$$Cl_2O_2 + ClO_2^- \rightarrow 2ClO_2(aq) + Cl^- \qquad (R18)$$

R17 would involve an initial nucleophilic attack on the hypochlorous acid followed by the addition of acid on the transient complex to eliminate water and form the often-postulated asymmetric Cl_2O_2 intermediate[34] with a Cl−Cl bond. The R17 + R18 pathway is extremely important in the rationalization of nonlinear autocatalytic kinetics in any oxidations involving chlorite.[34] Any two-electron oxidation by the intermediate species should result in the formation of two molecules of the reactive intermediate, HOCl:

$$Cl_2O_2 + 2e^- + 2H^+ \rightarrow 2HOCl \qquad (R19)$$

or specifically:

$$Cl_2O_2 + NAC{-}CH_2SH + H_2O \rightarrow 2HOCl + NAC{-}CH_2SOH \qquad (R20)$$

If the bulk of the oxidation is carried out by HOCl, then quadratic autocatalysis is easily justified by the tandem of R17 + R18. Figures 2, 3, and 4 show some mild autocatalysis in chlorine dioxide formation. This less than assertive autocatalytic production of chlorine dioxide can be traced to other reactions in solution which are concomitantly consuming chlorine dioxide concurrently with its autocatalytic production. Figures 5a−c show that, indeed, this is the case. After formation of HOCl in reaction R12, we would expect the series of reactions:

$$NAC{-}CH_2SOH + HOCl \rightarrow NAC{-}CH_2SO_2H + Cl^- + H^+ \qquad (R21)$$

$$NAC{-}CH_2SO_2H + HOCl \rightarrow NAC{-}CH_2SO_3H + Cl^- + H^+ \qquad (R22)$$

$NAC{-}CH_2SO_3H$, cysteic acid, is the final product in this oxidation. Reactions R21 and R22 can be written with ClO_2^- and/or $Cl_2(aq)$ as the oxidants:

$$NAC{-}CH_2SOH + ClO_2^- + H^+ \rightarrow NAC{-}CH_2SO_2H + HOCl \qquad (R23)$$

$$NAC{-}CH_2SOH + Cl_2(aq) + H_2O \rightarrow NAC{-}CH_2SO_2H + 2Cl^- + 2H^+ \qquad (R24)$$

where reactions R23 and R24 have been written as composites of two steps in each reaction. The most important reaction step in the whole mechanism is the formation of the reactive species, HOCl (e.g., reactions of the type R12, R13 + R14, and R23). All the observed nonlinearities can be traced to HOCl production.

Figure 2 (and to an extent, Figure 4 as well) show what appears to be uneven chlorine dioxide formation (a slower rate followed by a more rapid production). Figure 3 does not show this "kink" in chlorine dioxide formation, but only a simple very rapid production followed by a rapidly attained plateau in chlorine dioxide concentrations. The "kink" would represent the

complete consumption of the organic substrate, subsequently resulting in the formation of chlorine dioxide only without its consumption. Data in Figure 3 were collected at excess oxidant, with a $[ClO_2^-]_0/[NAC-CH_2SH]_0$ ratio of 10. At such overwhelming excess of oxidant, the reductant is consumed almost instantly, resulting in the observation of reaction R10 only. The substrate, in this case, acts as a mere catalyst for the production of chlorine dioxide from chlorite. The same scenario had been observed by us on the reaction between chlorite and formaldehyde.[31]

Reactions of Chlorine Dioxide. The direct reaction of chlorine dioxide with *N*-acetylcysteine appears to be a straightforward bimolecular reaction that is inhibited by acid (see Figure 5a−c). Chlorine dioxide is a radical species that oxidizes via a one-electron transfer to the chlorine atom to form the more stable chlorite:

$$ClO_2(aq) + e^- \rightarrow ClO_2^- \qquad (R25)$$

$$ClO_2^- + H^+ \rightleftharpoons HClO_2 \quad K_a^{-1} \qquad (R26)$$

Any other oxychlorine species formed, apart from chlorous acid, will be less energetically stable in mild to strongly acidic media. The formation of chlorous acid reduces the mechanism to the one described above of the main reaction under study: ClO_2^-−*N*-acetylcysteine. One might then expect oligooscillatory chlorine dioxide formation from them, but the high initial chlorine dioxide content, coupled with low chlorite concentrations ensures that we observe a steady and monotonic decrease in chlorine dioxide during the duration of the whole reaction.

A one-electron oxidation of *N*-acetylcysteine should produce thiyl radicals which should be energetically unfavored in this aqueous acidic reaction medium:

$$ClO_2(aq) + NAC-CH_2SH \rightleftharpoons ClO_2^- + NAC-CH_2S^\bullet + H^+ \qquad (R27)$$

The general propensity of the thiyl radical is to dimerize to form a disulfide:

$$2NAC-CH_2S^\bullet \rightarrow (NAC-CH_2S\text{-})_2(s) \qquad (R28)$$

In aqueous media, we expect this dimer to be extremely unstable and to also precipitate out of solution. Since no precipitation was observed in this reaction system, we discount the R27 + R28 pathway as being viable. Instead, we invoke a previous pathway which was postulated for L-cysteine which involves the initial formation of an intimate adduct of *N*-acetylcysteine with chlorine dioxide:

$$NAC-CH_2SH + ClO_2(aq) \rightleftharpoons [NAC-CH_2S-ClO_2]^- + H^+ \qquad (R29)$$

This adduct is very easy to form from the electron-rich thiol center and the radical chlorine center. The adduct can either dissociate back to the reactants or collide with another chlorine dioxide molecule to form products:

$$[NAC-CH_2S-ClO_2]^{-\bullet} H^+ + ClO_2(aq) + H_2O \rightarrow NAC-CH_2SOH + 2HClO_2 \qquad (R30)$$

Reaction kinetics suggest that the formation of the adduct is the rate-determining step. If R30 had been rate-determining, then the rate law would have been second order in chlorine dioxide. Further oxidation can be effected by either chlorite, chlorous acid, or hypochlorous acid.

$$NAC-CH_2SH + HClO_2 \rightarrow NAC-CH_2SOH + HOCl \qquad (R31)$$

Acid effect will be observed if the rate of reaction R13 is different from that of R31. This effect, however, will be observed only in the neighborhood of reaction medium pH that equals the pK_a of chlorous acid which is approximately 2.0. Below pH 2.0 one does not expect large changes in the $[ClO_2^-]_0/[HClO_2]_0$ ratio as the chlorine (III) species will be predominantly in the protonated chlorous acid form. From purely electrostatic considerations, reaction R31 should be faster than R13; and this would run counter to the observed acid dependence data (Figure 5c). Thus, the protolytic equilibrium R26 is not responsible for the observed acid retardation in the reaction of chlorine dioxide and *N*-acetylcysteine.

The electron-rich thiol group in *N*-acetylcysteine can be protonated in highly acidic conditions, thereby reducing its nucleophilic capabilities.

$$NAC-CH_2SH + H^+ \rightleftharpoons [NAC-CH_2SH_2]^+ \quad K_b \qquad (R32)$$

While the protonated thiol formed in R32 can react faster with chlorite (R13) than with $HClO_2$ (R26), the pH values that support protonated thiol do not support chlorite, and so those types of reactions can be ignored in this mechanism. The rate of reaction, as measured by the rate of disappearance of chlorine dioxide, will be given by

$$\frac{-d[ClO_2]}{dt} = k_{29}[NAC-CH_2SH][ClO_2(aq)] \qquad (1)$$

Acid inhibition can be rationalized by assuming inertness of the protonated thiol. By using this assumption, one can derive the following rate law from eq 1 for the rate of reaction between *N*-acetylcysteine and chlorine dioxide:

$$\frac{-d[ClO_2]}{dt} = \frac{k_{29}}{1 + K_b[H^+]}\{[NAC-CH_2SH]_0[ClO_2(aq)]\} \qquad (2)$$

There is no real established value of K_b for the thiol group of *N*-acetylcysteine due to the zwitterionic species resident on the asymmetric carbon center. The value of k_{29}, the direct reaction of chlorine dioxide with *N*-acetylcysteine was evaluated from this study as $600 \pm 50\ M^{-1}\ s^{-1}$.

Overall Reaction Network. We can produce a minimal set of reactions needed to fully explain the data we obtained for this reaction. The absence of oligooscillatory behavior with respect to chlorine dioxide formation can allow us to drop the autocatalytic production of HOCl. All we need to do to justify all the observed reaction dynamics is to construct a mechanism that can include reactions R9−R11. This mechanism is shown in Table 1. This mechanism involves 5 oxyhalogen−sulfur reactions (which were considered irreversible), one pure oxyhalogens reaction (M2) and two rapid protolytic equilibria. Using this simplified scheme, we were able to successfully model the data shown in Figures 2 and 3. By shutting down reaction M8, we were also able to simulate the acid dependence data shown in Figure 5c for the oxidation of *N*-acetylcysteine by chlorine dioxide.

TABLE 1: Concise Mechanism for the *N*-Acetylcysteine−Chlorite Reaction

reaction number	reaction[a]	k_f; k_r[b]
M1	$NAC-CH_2SH + ClO_2^- + H^+ \rightarrow HOCl + NAC-CH_2SOH$	125
M2	$HOCl + 2ClO_2^- + H^+ \rightleftharpoons 2ClO_2(aq) + Cl^- + H_2O$	1.01×10^6, 1×10^2
M3	$NAC-CH_2SH + HOCl \rightarrow NAC-CH_2SOH + Cl^- + H^+$	7.5×10^3
M4	$NAC-CH_2SOH + HOCl \rightarrow NAC-CH_2SO_2H + Cl^- + H^+$	1×10^4
M5	$NAC-CH_2SO_2H + HOCl \rightarrow NAC-CH_2SO_3H + Cl^- + H^+$	4×10^3
M6	$NAC-CH_2SH + 2ClO_2(aq) \rightarrow NAC-CH_2SOH + 2ClO_2^- + 2H^+$	600 (M^{-1} s^{-1})
M7	$NAC-CH_2SH + H^+ \rightleftharpoons [NAC-CH_2SH_2]^+$	1×10^3; 5×10^9
M8	$H^+ + ClO_2^- \rightleftharpoons HClO_2$	1×10^9; 1.02×10^7

[a] Legend: $NAC-CH_2SH$, *N*-acetylcysteine; $NAC-CH_2SOH$, *N*-acetylcysteinesulfenic acid. [b] Except where water is involved and for reaction M6, the units for the rate constant are derived from the molecularity of the reaction.

Bromate Oxidation of *N*-Acetylcysteine. The data in Figures 6−9 show no oligooscillatory behavior, only a simple reaction that shows an induction period followed by a very sharp and sudden formation of aqueous bromine. Bromine is formed by the reaction of bromate and bromide in acidic medium as shown in reaction R4. The needed bromide is formed from the reduction of bromate by *N*-acetylcysteine. The dynamics observed in this reaction scheme do not differ much from those obtained from the oxidation of pure DL-cysteine by acidic bromate.[21] The sharp end of the induction period suggests that the reaction of bromine with *N*-acetylcysteine and its metabolites must be very fast. The data in Figure 9 prove this assertion: the reaction of bromine and *N*-acetylcysteine is so rapid that it is nearly over within the mixing time of our stopped-flow spectrophotometer. These data shows that our stopped-flow spectrophotometer only catches the last 30% of the reaction. The majority of the bromine is consumed within the mixing and pre-triggering time of the spectrophotometer. The formation of bromine in Figures 6−8 can be used as an indicator reaction which can show us that all the reducing substrates in solution will have been completely consumed. Consequently, the time taken for the consumption of the reducing substrates in solution can be related to the rate of the bromate−*N*-acetylcysteine reaction. For a fixed amount of *N*-acetylcysteine, the inverse of the induction period should be directly proportional to the rate of reaction. A plot of the square of the acid concentrations against the inverse of the induction period for the data shown in Figure 6a gives a straight line which indicates that the reaction which consumes *N*-acetylcysteine is dependent on acid to its second power. The same treatment for the data in Figure 6b shows a linear dependence of the initial bromate concentrations to the inverse of the induction period; meaning a first-order dependence of the reaction on bromate concentrations. Data in Figure 7a confirm our assertion that consumption of *N*-acetylcysteine is a prerequisite for the formation of bromine: at low ratios of oxidant to reductant (e.g., circa the stoichiometric equivalents), addition of *N*-acetylcysteine increases the induction period. Data taken, however, at overwhelming excess of oxidant, show an invariant induction period, with the only difference appearing in the rate of formation of bromine after the induction period (higher *N*-acetylcysteine concentrations gave more rapid bromine formation).

These data suggest the dominance of oxybromine kinetics in the overall reaction dynamics with the substrate playing a catalytic role. From Figures 6a and b, one can deduce that the overall reaction kinetics are second order in acid and first order in bromate. The effect of the substrate can be evaluated from the data in Figure 7b. Despite an invariant induction period, the rates of formation of bromine at the end of the induction period is directly proportional to the initial concentration of *N*-acetylcysteine. The rate law for the rate of consumption of *N*-acetylcysteine can be deduced from these data to be

$$-d[NAC-CH_2SH]/dt = k_0[BrO_3^-][NAC-CH_2SH][H^+]^2 \quad (3)$$

The initial step must involve a protonation of the bromate anion to form bromic acid:

$$H^+ + BrO_3^- \rightleftharpoons HBrO_3 \quad (R33)$$

Bromic acid will next react with the thiol to produce unstable bromous acid and equally unstable sulfenic acid, $NAC-CH_2SOH$:

$$HBrO_3 + NAC-CH_2SH \rightarrow HBrO_2 + NAC-CH_2SOH \quad (R34)$$

In the absence of bromide, bromous acid will rapidly disproportionate:

$$2HBrO_2 \rightleftharpoons HOBr + BrO_3^- + H^+ \quad (R35)$$

Hypobromous acid is extremely reactive and will react with any reducing agent in solution to produce bromide:

$$HOBr + NAC-CH_2SH \rightarrow NAC-CH_2SOH + H^+ + Br^- \quad (R36)$$

The emergence of the bromide will facilitate the formation of more reactive oxybromine species:

$$BrO_3^- + 2H^+ + Br^- \rightarrow HBrO_2 + HOBr \quad (R37)$$

At this point, reaction R37 becomes the rate-determining step. Even though the production of bromide is controlled by initiation reaction R34, since the production of bromide is autocatalytic, control of the reaction is effectively passed onto reaction R37. This can be rationalized from the addition of reactions R34 + R35 + 2R36 + R37 which gives the simple stoichiometric equation that is autocatalytic in bromide:

$$BrO_3^- + 3NAC-CH_2SH + Br^- \rightarrow 3NAC-CH_2SOH + 2Br^- \quad (R38)$$

Further oxidation will occur in a stepwise process until *N*-acetylcysteic acid, $NAC-CH_2SO_3H$, is formed:

$$HOBr + NAC-CH_2SOH \rightarrow NAC-CH_2SO_2H + H^+ + Br^- \quad (R39)$$

$$HOBr + NAC-CH_2SO_2H \rightarrow NAC-CH_2SO_3H + H^+ + Br^- \quad (R40)$$

TABLE 2: Mechanism for the Bromate−*N*-Acetylcysteine Reaction in Acidic Media

number	reaction	k_f; k_r
P1	$H^+ + BrO_3^- \rightleftharpoons HBrO_3$	1×10^7; 1×10^9
P2	$HBrO_3 + NAC{-}CH_2SH \rightarrow HBrO_2 + NAC{-}CH_2SOH$	5×10^2
P3	$2HBrO_2 \rightleftharpoons HOBr + BrO_3^- + H^+$	4×10^7; 2×10^{-10}
P4	$HOBr + Br^- + 2H^+ \rightleftharpoons Br_2(aq) + H_2O$	8×10^9; 110
P5	$BrO_3^- + 2H^+ + Br^- \rightleftharpoons HBrO_2 + HOBr$	2.1; 1×10^4
P6	$HBrO_2 + Br^- + H^+ \rightleftharpoons 2HOBr$	2×10^9; 5×10^{-5}
P7	$HOBr + NAC{-}CH_2SH \rightarrow NAC{-}CH_2SOH + H^+ + Br^-$	5×10^6
P8	$HOBr + NAC{-}CH_2SOH \rightarrow NAC{-}CH_2SO_2H + H^+ + Br^-$	5×10^5
P9	$HOBr + NAC{-}CH_2SO_2H \rightarrow NAC{-}CH_2SO_3H + H^+ + Br^-$	1×10^4
P10	$Br_2(aq) + NAC{-}CH_2SH + H_2O \rightarrow NAC{-}CH_2SOH + 2H^+ + 2Br^-$	5×10^7
P11	$Br_2(aq) + NAC{-}CH_2SOH + H_2O \rightarrow NAC{-}CH_2SO_2H + 2H^+ + 2Br^-$	2.5×10^6
P12	$Br_2(aq) + NAC{-}CH_2SO_2H + H_2O \rightarrow NAC{-}CH_2SO_3H + 2H^+ + 2Br^-$	1×10^3

At each oxidation step, more bromide is formed, further establishing reaction R37 as the bottleneck and rate-determining step. The rate law of reaction R37 is well-known:

$$-d[BrO_3^-]/dt = k_0[BrO_3^-][Br^-][H^+]^2 \quad (4)$$

One can map the bromide in eq 4 with *N*-acetylcysteine in eq 3 since the rate of production of bromide is controlled by reaction R34, which in turn is dependent on the concentration of *N*-acetylcysteine; hence, the overall rate law for the reaction is eq 3.

Formation of Bromine. Having established the very rapid reaction of bromine with the substrate, we can assume that formation of bromine is controlled by reaction R37 after all the reducing species in solution have been consumed. One of the most rapid reactions in the reaction mixture is the reverse of the hydrolysis of bromine.[32]

$$HOBr + Br^- + 2H^+ \rightleftharpoons Br_2(aq) + H_2O \quad k_f = 8 \times 10^9\ M^{-2}\ s^{-1} \quad (R41)$$

The reaction of bromine with substrate, however, is faster and diffusion-limited.

$$Br_2(aq) + NAC{-}CH_2SH + H_2O \rightarrow NAC{-}CH_2SOH + 2H^+ + 2Br^- \quad (R42)$$

Reaction R41 is the only route by which bromine is formed; as long as reactions of type R42 mop up all the bromine as soon as it is formed, there will be no accumulation of bromine and the induction period will persist. When bromine production finally commences, its rate of formation will depend on the available excess bromate (after being depleted by *N*-acetylcysteine), bromide, and acid. The acid concentrations used in these experiments were so high that the pH of the reaction medium did not change much for the duration of the reaction. If we assume quantitative production of bromide according to stoichiometry R3, then the concentration of available bromide will equate to the initial *N*-acetylcysteine concentrations. Thus we can justify data observed in Figure 7b where the rate of formation of bromine after the induction period is directly proportional to the initial reductant concentration.

Effect of Bromide. Availability of bromide at $t = 0$ will shunt the processes that initially form $HBrO_2$ and HOBr. One would expect an acceleration of the rate of reaction on the basis of a shorter induction period as well as enhanced rate and production of bromine. The most important reaction that will asset itself when bromide is present is the formation of hypobromous acid from bromous acid:

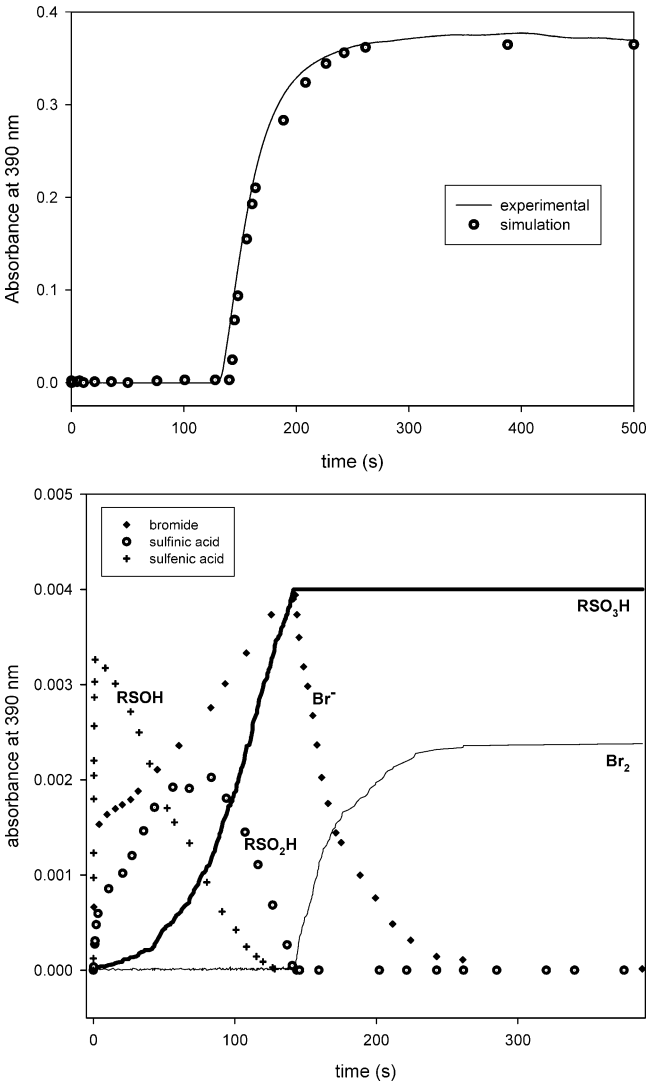

Figure 10. (a) Computer simulations using the mechanism shown in Table 2 for the acid dependence of the bromate−*N*-acetylcysteine reaction. $[NAC{-}CH_2SH]_0 = 0.004$ M. $[H^+]_0 = 0.67$ M. $[BrO_3^-]_0 = 0.01$ M. The model also correctly predicted the bromate and bromide dependences shown in Figures 6b and 8. (b) Modeling of some of the species that could not be experimentally determined. Reaction conditions are the same as those in Figure 10a. Full consumption of the sulfenic and sulfinic acids is necessary before production of bromine can begin. Bromide rises to a maximum before falling to produce bromine from bromate.

$$HBrO_2 + Br^- + H^+ \rightleftharpoons 2HOBr \quad k_f = 2 \times 10^9\ M^{-2}\ s^{-1} \quad (R43)$$

Combining reactions R37 and R43 will show an overall stoichiometry at the beginning of the reaction which produces

more reactive species and accelerates the reaction:

$$BrO_3^- + 3H^+ + 2Br^- \rightleftharpoons 3HOBr \qquad (R44)$$

Since it has been established that further reaction of HOBr to form bromide is fast, then R44 exhibits cubic autocatalysis in bromide. Small, trace and catalytic amounts of bromide will display a very significant catalytic effect due to enhancement of reaction R44, but further increases in initial bromine concentrations should show a saturation as reaction R37 will take over from $t = 0$ as the rate-determining step. The data in Figure 8 show this trend quite distinctly. There is a dramatic shortening of the induction period between trace a (no added bromide), and trace b (0.0002 M Br^-), and a less dramatic effect as more bromide is subsequently added.

Computer Simulations. The whole reaction can be adequately described by a network of only 12 reactions shown in Table 1. The reaction scheme shown has one protolytic equilibrium (reaction P1), 4 standard oxybromine reactions, and 8 oxybromine−organosulfur reactions. These 12 reactions represent a very simplified reaction scheme in which we have taken advantage of the rapid reaction M6 to ignore any other oxidants in the reaction mixture apart from HOBr and Br_2. The rate constants for the 4 oxybromine reactions were taken from literature values,[35−37] and the only important kinetics parameters in the mechanism turned out to only be those for reactions P2 and P7. The kinetics parameters for reaction P1 are known to be diffusion-controlled. The use, however, of diffusion-controlled rate constants increased the degree of stiffness of the integration. The forward and reverse constants used for P1 were chosen such that the accepted value for the acidity constant of bromic acid was maintained ($pK_a \approx -0.5$).[38] The rate constant used for reaction P2 was based on the best fit of the data to the induction period. Kinetics parameters for reactions P10, P11, and P12 were estimated from this study. The rate laws were derived from the molecularity of the reactions except where water was involved in which it was taken as the solvent with an activity, $a = 1$. Figure 10a shows a very good fit to the data using this simplified mechanism. Figure 10b shows the concentration variations of the different intermediate species which we could not experimentally determine. Both the sulfenic and sulfenic acids accumulate to some maxima before being consumed to form the sulfonic acid. Bromine is formed as soon as these transient oxo-acids have been consumed. Bromide, as expected, accumulates during the time when reducing substrates are still available, and gradually falls to zero in excess bromate conditions through reaction P4 to satisfy stoichiometry R5.

Conclusion

Despite the vast differences in the physiological effects of cysteine and *N*-acetylcysteine, it would appear that their S-oxygenation mechanisms are very similar; differing only in the rates of oxidation. The acetyl group must play a structural and inductive role only.

Acknowledgment. We thank the University of the Western Cape, Bellville, South Africa, for granting leave of absence to one of us (J.D.). This work was supported by Grant CHE 0137435 from the National Science Foundation.

References and Notes

(1) Parcell, S. *Altern. Med. Rev.* **2002**, *7*, 22−44.
(2) Lauterburg, B. H. *Am. J. Ther.* **2002**, *9*, 225−233.
(3) Murray, M. F.; Langan, M.; MacGregor, R. R. *Nutrition* **2001**, *17*, 654−656.
(4) Droge, W. *Pharmacology* **1993**, *46*, 61−65.
(5) Roederer, M.; Staal, F. J.; Ela, S. W.; Herzenberg, L. A.; Herzenberg, L. A. *Pharmacology* **1993**, *46*, 121−129.
(6) Walmsley, S. L.; Khorasheh, S.; Singer, J.; Djurdjev, O. *J. Acquired Immune Defic. Syndr. Hum. Retrovirol.* **1998**, *19*, 498−505.
(7) Chapple, I. L. *J. Clin. Periodontol.* **1997**, *24*, 287−296.
(8) Kondo, M.; Oya-Ito, T.; Kumagai, T.; Osawa, T.; Uchida, K. *J. Biol. Chem.* **2001**, *276*, 12076−12083.
(9) Yang, Q.; Hergenhahn, M.; Weninger, A.; Bartsch, H. *Carcinogenesis* **1999**, *20*, 1769−1775.
(10) Ferrandiz, M. L.; Bustos, G.; Paya, M.; Gunasegaran, R.; Alcaraz, M. J. *Life Sci.* **1994**, *55*, L145−L150.
(11) Suntres, Z. E. *Toxicology* **2002**, *180*, 65−77.
(12) Lugo-Vallin, N. V.; Pascuzzo-Lima, C.; Maradei-Irastorza, I.; Ramirez-Sanchez, M.; Sosa-Sequera, M.; Aguero-Pena, R.; Granado-Duque, A. *Vet. Hum. Toxicol.* **2002**, *44*, 40−41.
(13) Roberts, R. L.; Aroda, V. R.; Ank, B. J. *J. Infect. Dis.* **1995**, *172*, 1492−1502.
(14) Hoffer, L. J. *Curr. Opin. Clin. Nutr. Metab. Care* **2002**, *5*, 511−517.
(15) Dringen, R.; Hamprecht, B. *Neurosci. Lett.* **1999**, *259*, 79−82.
(16) Flanagan, R. J.; Meredith, T. J. *Am. J. Med.* **1991**, *91*, 131S−139S.
(17) Breitkreutz, R.; Holm, S.; Pittack, N.; Beichert, M.; Babylon, A.; Yodoi, J.; Droge, W. *AIDS Res. Hum. Retroviruses* **2000**, *16*, 203−209.
(18) Droge, W.; Breitkreutz, R. *Curr. Opin. Clin. Nutr. Metab. Care* **1999**, *2*, 493−498.
(19) den Hartog, G. J.; Haenen, G. R.; Vegt, E.; van der Vijgh, W. J.; Bast, A. *Biol. Chem.* **2002**, *383*, 709−713.
(20) Peskin, A. V.; Winterbourn, C. C. *Free Radical Biol. Med.* **2001**, *30*, 572−579.
(21) Darkwa, J.; Mundoma, C.; Simoyi, R. H. *J. Chem. Soc., Faraday Trans.* **1998**, *94*, 1971−1978.
(22) Chinake, C. R.; Simoyi, R. H. *J. Phys. Chem.* **1994**, *98*, 4012−4019.
(23) Epstein, I. R.; Kustin, K.; Simoyi, R. H. *J. Phys. Chem.* **1992**, *96*, 6326−6331.
(24) Salem, M. A.; Chinake, C. R.; Simoyi, R. H. *J. Phys. Chem.* **1996**, *100*, 9377−9384.
(25) Csordas, V.; Bubnis, B.; Fabian, I.; Gordon, G. *Inorg. Chem.* **2001**, *40*, 1833−1836.
(26) Lopez-Cueto, G.; Ostra, M.; Ubide, C. *Anal. Chim. Acta* **2001**, *445*, 117−126.
(27) Chinake, C. R.; Simoyi, R. H. *Ach-Models Chem.* **1998**, *135*, 771−781.
(28) Fabian, I.; Szucs, D.; Gordon, G. *J. Phys. Chem. A* **2000**, *104*, 8045−8049.
(29) Peintler, G.; Nagypal, I.; Epstein, I. R. *J. Phys. Chem.* **1990**, *94*, 2954−2960.
(30) Chinake, C. R.; Simoyi, R. H.; Jonnalagadda, S. B. *J. Phys. Chem.* **1994**, *98*, 545−550.
(31) Chinake, C. R.; Olojo, O.; Simoyi, R. H. *J. Phys. Chem. A* **1998**, *102*, 606−611.
(32) Kustin, K.; Eigen, M. *J. Am. Chem. Soc.* **1962**, *84*, 1355−1359.
(33) Jia, Z.; Margerum, D. W.; Francisco, J. S. *Inorg. Chem.* **2000**, *39*, 2614−2620.
(34) Rabai, G.; Orban, M. *J. Phys. Chem.* **1993**, *97*, 5935−5939.
(35) Szalai, I.; Kurin-Csorgei, K.; Orban, M. *Phys. Chem. Chem. Phys.* **2002**, *4*, 1271−1275.
(36) Szalai, I.; Oslonovitch, J.; Forsterling, H. D. *J. Phys. Chem. A* **2000**, *104*, 1495−1498.
(37) Szalai, I.; Koros, E. *J. Phys. Chem. A* **1998**, *102*, 6892−6897.
(38) Sortes, C. E.; Faria, R. B. *J. Braz. Chem. Soc.* **2001**, *12*, 775−779.